

**Supplementary methods:**

*Isolation and culture of primary murine and human MSCs and leukemia cells lines.* Viability of all cell types isolated from wild-type and CTGF knockout mice was tested by the Trypan blue dye exclusion method. Cell suspensions were cultured in tissue culture flasks at an initial density of  $1 \times 10^6$  cells/cm<sup>2</sup> flasks in the presence of alpha-MEM containing 20% FBS. The cultures were inspected for growth of colony forming units-fibroblast-like (CFU-F) representing MSCs. Human MSCs were isolated from the BM of healthy donors undergoing BM harvest for use in allogeneic transplantation as described earlier(1). All BM donors provided written informed consent, and this study was conducted according to institutional guidelines under an approved protocol. Acute lymphoid leukemia (ALL) cell lines, including Jurkat (T-cell ALL), REH (pre-B-cell ALL), RS4;11 (B-cell ALL), and Nalm6 (B-cell ALL), and AML cell line Molm13 were purchased from ATCC and cultured as per ATCC recommendation in RPMI (Media Tech, Inc.) with 10% FBS and 1% penicillin–streptomycin.

*CTGF knockdown by lentiviral transduction.*

In brief, 293T cells were co-transfected with pMD2.G and psPAX2 (Addgene, Inc.), along with a lentiviral construct expressing either a specific *CTGF*-shRNA or the empty vector as control, using JetPrime transfection reagent (Polyplus, Polyplus, Berkeley, CA). MSCs were then transduced with a viral supernatant derived from empty lentiviral or *CTGF*-shRNA–expressing vector. MSCs were cultured for 5 days in selection medium (2 $\mu$ g/ml puromycin, Invitrogen, Grand Island, NY), which was then replaced with complete cell culture medium rendering the cells ready for experimental use.

*Western blot analysis.* Cells were subjected to lysis at a density of  $3 \times 10^5/50 \mu\text{l}$  in protein lysis buffer (0.25 M Tris-HCl, 2% SDS, 4%  $\beta$ -mercaptoethanol, 10% glycerol, and 0.02% bromophenol blue) supplemented with a protease inhibitor cocktail (Roche Diagnostic Co., Indianapolis, IN). Cell lysates were loaded onto a 10% polyacrylamide gel (Bio-Rad, Hercules, CA) for electrophoresis, and the proteins were then transferred to Immobilon-FL membranes (Millipore, Billerica, MA). The membranes were incubated with goat anti-human CTGF antibody (Santa Cruz Biotechnology, SantaCruz, CA) and mouse anti-human tubulin antibody (Sigma-Aldrich) overnight at  $4^\circ\text{C}$ , washed and incubated with donkey-anti-mouse IgG antibody conjugated with Alexafluor-700 and donkey-anti-goat antibody conjugated with Alexafluor-800 (both from Invitrogen). Membranes were washed again and scanned using the Odyssey fluorescence imaging system (LI-COR Biosciences, Lincoln, Nebraska, USA).

*Flow cytometry:* The following antibody conjugates were used: anti-CD44 antibody conjugated with allophycocyanin (APC) and anti-CD90 and anti-CD105 antibodies conjugated with PE were purchased from eBiosciences (San Diego, CA), and anti-CD140b, anti-CD146, anti-CD73, anti-CD166, anti-CD14, and anti-CD140b conjugated with PE and anti-CD45 conjugated with FITC were purchased from BD Biosciences (San Jose, CA). After incubation, the cells were washed with FACS buffer containing  $0.5 \mu\text{g/ml}$  DAPI (to exclude dead cells) and analyzed on an LSR-II Flow Cytometer. Ten thousand events were acquired for each sample. The flow cytometric data were analyzed by FCS Express software (Denovo Software, Los Angeles, CA).

*Real-time RT-PCR.* Human GAPDH was used as an equal loading control. The PCR primers used to amplify human genes by the SYBR green method included CTGF and leptin, (CTGF

forward: 5'GGGAAATGCTGCGAGGAGTG3', CTGF reverse:  
5'CAGGCGCTCCACTCTGTGGTC3'; Leptin forward: 5' CCAAACCCTCATCAAGAC3',  
Leptin reverse: 5' GGAGCCCAGGAATGAAGTCC3'; GAPDH forward: 5'  
GCCAAGGTCATCCATGACAACCTTTGG3', GAPDH reverse:  
5'GCCTGCTTCACCACCTTCTTGATGTC3'). Primers used in the TaqMan-based qRT-PCR  
assay, including CTGF, Cyr61, Nov, WISP1, WISP2, and LRP1, were purchased from Applied  
Biosystems (Foster City, CA). Real-time PCR was carried out in an ABI Prism 7900 HT  
instrument (Applied Biosystems) as described earlier(1).

*Gene expression analysis:* Significance testing for differentially-expressed probes was by the  
Wilcoxon rank-sum test applied to individual processed bead values, with false-discovery rate  
significance values (q) determined by the method of Benjamini and Hochberg(2). Hierarchical  
clustering and heat mapping used Cluster and Treeview software from Eisen et al(3). Gene set  
analysis applied gene set enrichment analysis (GSEA)(4) and the hypergeometric distribution  
test(5) to gene sets from mSigDB and individual literature sources. Statistical significance was  
assessed at the .05 level.

*Multi-lineage differentiation:* To determine alkaline phosphatase activity, cells were incubated  
with FAST BCIP/NBT substrate (Sigma-Aldrich) for 20 minutes at room temperature. Calcium  
deposition was analyzed by staining with 1% Alizarin Red S (Spectrum, Gardena, CA) for 5  
minutes at room temperature. After the cells were washed, they were photographed by a Nikon  
Coolpix-950 camera attached to a Nikon-TMS light microscope. The formation of adipocytes was  
evaluated by fixing cells with 4% PFA and staining with Oil Red O dye (Sigma-Aldrich) for 15  
minutes at room temperature. As an alternative, oil droplets were also stained using LipidTox, a

fluorescent lipid dye from Invitrogen. Oil Red O–stained cells were pictured by a Nikon Coolpix-950 camera attached to a Nikon-TMS light microscope, and LipidTox stained cells were pictured by an inverted fluorescent microscope (Olympus, Center Valley, PA). To visualize chondrocyte differentiation, the cell pellets were fixed with 3.7% formalin, embedded in paraffin, and cut into 5- $\mu$ m sections. Following deparaffinization and hydration, sections were incubated with Alcian Blue 8GX solution (Sigma-Aldrich) for 30 minutes at room temperature, and slides were washed in 3% acetic acid and then in distilled water. Photographs were taken by a Olympus DP72 digital camera attached to a BX43 microscope (Olympus America, Inc).

*Generation of the acute myeloid/lymphoid leukemia model.* Briefly, mice were anesthetized and, 5 minutes prior to imaging, each mouse was given an intraperitoneal injection of D-luciferin (125 mg/kg; Biotium, Hayward, CA) and imaged noninvasively with the in vivo Xenogen IVIS-200 bioluminescence/fluorescence optical imaging system. Two weeks after transplantation of leukemia cells, mice were humanely killed by CO<sub>2</sub> asphyxiation. Optical images were displayed and analyzed by the IVIS Living Image 200 software (Caliper Life Sciences). The luminescent signal intensity of each EXM-BM was quantified by manually drawing regions of interest (ROI) using the IVIS Living Image 200 software tool and total photon flux from each mouse from the same group was pooled to obtain an average signal(1, 6).

*Immunohistochemical analysis.* The extent of leukemic infiltration in murine tissues was assessed by staining with hematoxylin and eosin (H&E, Sigma-Aldrich) and by immunohistochemical analysis with an anti-luciferase antibody (Promega) for firefly luciferase–positive leukemic cells. Fresh tissues collected from mice were fixed in 4% PFA and

embedded in paraffin. Sections (5  $\mu\text{m}$ ) were stained with H&E and analyzed by light microscopy. For immunohistochemical staining, the tissue sections were first boiled in 1 $\times$  antigen retrieval buffer (DAKO, Carpinteria, CA) for 20 minutes and, after washing, were incubated for 30 minutes in serum-free blocking solution (DAKO) and then overnight with 1:100 dilution of anti-C/EPB $\alpha$  (Abcam, Cambridge, MA) or anti-PPAR $\gamma$  (Abcam) or anti-leptin (Abcam) or anti-firefly luciferase (Promega) or an isotype control antibody. The tissue sections were then sequentially incubated with a biotinylated antibody and peroxidase-labeled streptavidin (DAKO). The staining was completed by incubation for 1 minute with DAB tetrahydrochloride/hydrogen peroxide, which results in a brown precipitate at the antigen site. The slides were photographed by an Olympus DP72 digital camera attached to a BX43 microscope (Olympus). For the human bone marrow biopsy specimens, the sections were formalin-fixed and formic acid-decalcified as described previously(7). Leptin expression was assessed using a rabbit-anti-human Leptin polyclonal antibody (Cone Ab16227, 1:200 dilution, overnight incubation with primary antibody). A specimen was considered positive if 10% or more of cells demonstrated cytoplasmic staining.

1. Battula, V.L., Evans, K.W., Hollier, B.G., Shi, Y., Marini, F.C., Ayyanan, A., Wang, R.Y., Briskin, C., Guerra, R., Andreeff, M., et al. 2010. Epithelial-mesenchymal transition-derived cells exhibit multilineage differentiation potential similar to mesenchymal stem cells. *Stem Cells* 28:1435-1445.
2. Benjamini, Y., and Hochberg, Y. 1995. Controlling the false discovery rate: a practical and powerful approach to multiple testing. *J Roy Stat Soc B* 57:289-300.
3. Eisen, M.B., Spellman, P.T., Brown, P.O., and Botstein, D. 1998. Cluster analysis and display of genome-wide expression patterns. *Proc Natl Acad Sci U S A* 95:14863-14868.
4. Subramanian, A., Tamayo, P., Mootha, V.K., Mukherjee, S., Ebert, B.L., Gillette, M.A., Paulovich, A., Pomeroy, S.L., Golub, T.R., Lander, E.S., et al. 2005. Gene set enrichment analysis: a knowledge-based approach for interpreting genome-wide expression profiles. *Proc Natl Acad Sci U S A* 102:15545-15550.

5. Jakt, L.M., Cao, L., Cheah, K.S., and Smith, D.K. 2001. Assessing clusters and motifs from gene expression data. *Genome Res* 11:112-123.
6. Zeng, Z., Shi, Y.X., Samudio, I.J., Wang, R.Y., Ling, X., Frolova, O., Levis, M., Rubin, J.B., Negrin, R.R., Estey, E.H., et al. 2009. Targeting the leukemia microenvironment by CXCR4 inhibition overcomes resistance to kinase inhibitors and chemotherapy in AML. *Blood* 113:6215-6224.
7. Konoplev, S., Rassidakis, G.Z., Estey, E., Kantarjian, H., Liakou, C.I., Huang, X., Xiao, L., Andreeff, M., Konopleva, M., and Medeiros, L.J. 2007. Overexpression of CXCR4 predicts adverse overall and event-free survival in patients with unmutated FLT3 acute myeloid leukemia with normal karyotype. *Cancer* 109:1152-1156.

**Supplementary Table-1:** Top 20 Gene Ontology (GO) biological process (BP) categories most significantly enriched by the hypergeometric distribution test among genes down-regulated in CTGF-KD-MSCs.

**Supplementary Table-2:** Cell proliferation related genes that are down regulated in CTGF-KD-MSCs. Samples 1 and 2 represents data derived from 2 independent experiments.

**Supplementary Figure 1:** ALL cell lines including Jurkat, REH and RS4;11 and human stromal cell line HS5 and BM derived MSCs were analyzed for expression of CTGF family members including CTGF, CYR61, NOV, WISP1, WISP2 and LRP1 by qRT-PCR. HS5 cell line and BM-MSCs express higher levels of these genes compared to ALL cell lines.

**Supplementary Figure 2: Cell surface expression of MSC related markers on control or CTGF-KD-MSCs.** Control or CTGF-KD-MSCs ( $1 \times 10^6$ ) were stained with anti-CD44 antibody conjugated with APC; anti-CD90, anti-CD105, anti-CD140b, anti-CD146, anti-CD73, anti-CD166, anti-CD14, or anti-CD140b antibody conjugated with PE; or anti-CD45 antibody conjugated with FITC. No differences in expression of cell surface proteins were observed. The stained cells were analysed on an LSR-II flow cytometer. The data were analyzed by FCS express software.

**Supplementary Figure 3: Knockdown of CTGF inhibits cell cycle of MSCs. (A&B)** Gene expression was analyzed on mRNA from control or CTGF-KD-MSCs by the Illumina microarray system. Gene set enrichment analysis was performed on the expression data derived

from microarray analysis, and genes involved in cell proliferation (A) or M phase of mitotic cell cycle (B) are represented in enrichment blots. (C) Cell cycle-related genes that were down regulated in CTGF-KD-MSCs (from 2 samples) are represented in an expression heat map developed with Cluster and TreeView software.

**Supplementary Figure 4. Differentiation of control or CTGF-KD-MSCs into osteoblasts or chondrocytes.** (A) Control- or CTGF-KD-MSCs ( $3 \times 10^4$ ) were cultured in the presence of osteoblast differentiation medium. After 3 weeks of incubation, the cells were fixed with 4% PFA. Osteoblast differentiation was measured by staining for alkaline phosphatase activity or mineral deposition by Alizarin Red S solution. (B) Cells ( $5 \times 10^5$ ) were cultured in chondrocyte differentiation medium for 4 weeks. The resulting pellets were fixed in 4% PFA and embedded in paraffin. The sections were then deparaffinized and stained using Alcian Blue dye.

**Supplementary Figure 5. Differentiation of control or CTGF-KD-MSCs into adipocytes.**  
Raw images of data displayed in Figure 3B

**Supplementary Figure 6. In vivo bone formation by control or CTGF-KD-MSCs.** Control or CTGF-KD-MSCs ( $1 \times 10^6$ ) in combination with EPCs (1:1 ratio) and Matrigel were transplanted subcutaneously in NOD/SCID/IL-2 $\gamma$ <sup>null</sup> mice. Eight weeks later, the mice were injected with OsteoSense fluorescent dye to analyze bone formation. The mice were imaged via the IVIS fluorescence imager.

**Supplementary Figure 7. Differentiation of normal- or AML- bone marrow derived MSCs into adipocytes.** To examine the differentiation potential of normal- or AML- bone marrow derived MSCs, cells ( $5 \times 10^4$ ) were cultured in adipocyte differentiation medium for 28 days. After incubation, the cells were stained by Oli Red O dye to observe adipocyte differentiation.

**Supplementary Table 1**

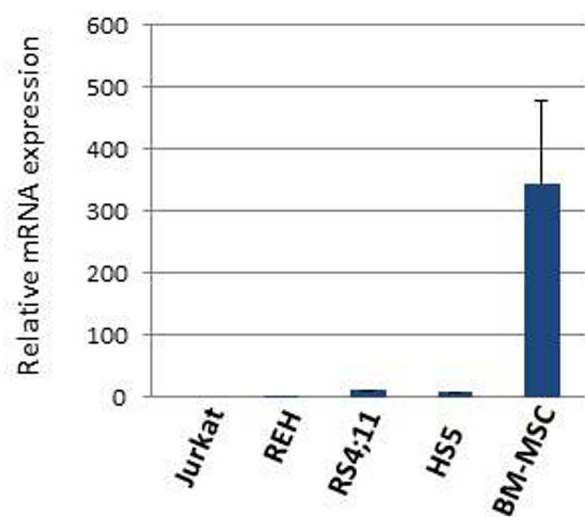
<u>Term_name</u>	<u>p value</u>	<u>q value</u>
M phase of mitotic cell cycle	0	0
mitosis	0	0
organelle fission	0	0
nuclear division	0	0
translational elongation	1.64E-13	5.63E-11
DNA replication	9.44E-13	2.70E-10
ribonucleoprotein complex biogenesis	3.08E-10	7.55E-08
ribosome biogenesis	7.08E-09	1.52E-06
microtubule cytoskeleton organization	2.03E-08	3.87E-06
chromosome segregation	3.93E-08	6.74E-06
RNA splicing	5.50E-07	8.58E-05
spindle organization	8.91E-07	0.000127354
rRNA processing	1.23E-06	0.000162523
microtubule-based process	2.56E-06	0.000308295
rRNA metabolic process	2.69E-06	0.000308295
organelle localization	1.02E-05	0.001089366
nucleic acid transport	1.56E-05	0.001404796
RNA transport	1.56E-05	0.001404796
establishment of RNA localization	1.56E-05	0.001404796
nucleobase, nucleoside, nucleotide and nucleic acid transport	2.07E-05	0.00177731

Supplementary Table 2

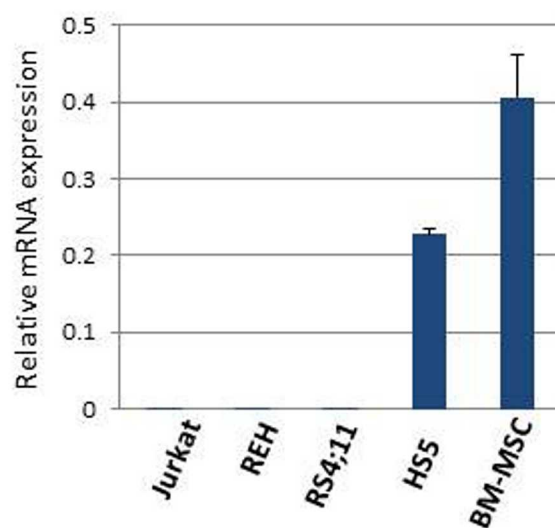
Gene Symbol	Sample 1	Sample 2	Gene Name
TCF7L1	0.3289795	-1.4002766	transcription factor 7-like 1 (T-cell specific, HMG-box)
NEK2	-0.1160402	-0.9536183	NIMA (never in mitosis gene a)-related kinase 2
LATS2	-0.3116216	-1.011233	LATS, large tumor suppressor, homolog 2 (Drosophila)
INCENP	-0.3313629	-1.1066513	inner centromere protein antigens 135/155kDa
BUB1	-0.4310887	-1.0972716	budding uninhibited by benzimidazoles 1 homolog (yeast)
ESPL1	-0.440958	-0.6257629	extra spindle pole bodies homolog 1 (S. cerevisiae)
HMGA2	-0.4993612	-0.5933316	high mobility group AT-hook 2
NCAPD3	-0.5361255	-0.4908654	non-SMC condensin II complex, subunit D3
KIFC1	-0.5361965	-0.8235	kinesin family member C1
ZWILCH	-0.5705496	-0.7735095	Zwilch, kinetochore associated, homolog (Drosophila)
ASPM	-0.5716567	-0.6430967	asp (abnormal spindle) homolog, microcephaly associated (Drosophila)
AURKA	-0.5756246	-0.6128809	aurora kinase A
CEP55	-0.6041603	-0.6344016	centrosomal protein 55kDa
NEK4	-0.6124028	-0.5745555	NIMA (never in mitosis gene a)-related kinase 4
KIF23	-0.6541145	-0.4955342	kinesin family member 23
NCAPG	-0.658811	-0.4730932	non-SMC condensin I complex, subunit G
UBE2C	-0.6602584	-0.8747988	ubiquitin-conjugating enzyme E2C
CDC25C	-0.7120742	-0.775082	cell division cycle 25 homolog C (S. pombe)
OIP5	-0.7126062	-0.9978674	Opa interacting protein 5
C13ORF34	-0.7274853	-0.3118904	chromosome 13 open reading frame 34
PRMT5	-0.7283726	-0.8520441	protein arginine methyltransferase 5
FAM83D	-0.7531203	-0.7410998	family with sequence similarity 83, member D
LMLN	-0.7666783	-0.6853239	leishmanolysin-like (metallopeptidase M8 family)
CDCA5	-0.7776483	-0.9604276	cell division cycle associated 5
NUSAP1	-0.7950104	-0.4710624	nucleolar and spindle associated protein 1
CDCA8	-0.801949	-0.8981122	cell division cycle associated 8
MAD2L1	-0.8199479	-0.2096344	MAD2 mitotic arrest deficient-like 1 (yeast)
CCNB2	-0.8322004	-0.8350035	cyclin B2
PLK1	-0.8366276	-1.2354191	polo-like kinase 1
RRS1	-0.852608	-0.3640492	RRS1 ribosome biogenesis regulator homolog (S. cerevisiae)
CENPE	-0.8566614	-0.8137523	centromere protein E, 312kDa
KIF2C	-0.8599514	-0.6838456	kinesin family member 2C
CENPF	-0.8716561	-0.3413738	centromere protein F, 350/400kDa (mitosin)
RCC1	-0.8875066	-0.6876737	regulator of chromosome condensation 1
CCDC99	-0.9025705	-0.6856064	coiled-coil domain containing 99
ANLN	-0.9205648	-0.8033802	anillin, actin binding protein
CLASP2	-0.9313297	-0.2234528	cytoplasmic linker associated protein 2
CDCA3	-0.9334859	-1.3305026	cell division cycle associated 3
ZWINT	-0.9390841	-0.8482054	ZW10 interactor
PTTG1	-0.9582124	-0.3027083	pituitary tumor-transforming 1
CCNA2	-1.002452	-0.8038101	cyclin A2
SGOL1	-1.0187189	-0.3414661	shugoshin-like 1 (S. pombe)
CDC20	-1.039473	-1.018815	cell division cycle 20 homolog (S. cerevisiae)
SPC25	-1.111242	-0.7171911	SPC25, NDC80 kinetochore complex component, homolog (S. cerevisiae)
CCNG1	-1.126861	-0.2242124	cyclin G1
CCNB1	-1.2443347	-1.0587025	cyclin B1
NCAPG2	-1.3341915	-1.1138389	non-SMC condensin II complex, subunit G2
TTK	-1.3455234	-1.3126233	TTK protein kinase
FBXO5	-1.3762267	-0.813725	F-box protein 5
SKA2	-0.749955902	-0.453789829	spindle and kinetochore associated complex subunit 2
ERCC6L	-0.974145582	-0.150264084	excision repair cross-complementing rodent repair deficiency, complementation group 6-like
CDK1	-1.062860579	-0.746682042	cyclin-dependent kinase 1

# Supplementary figure -1

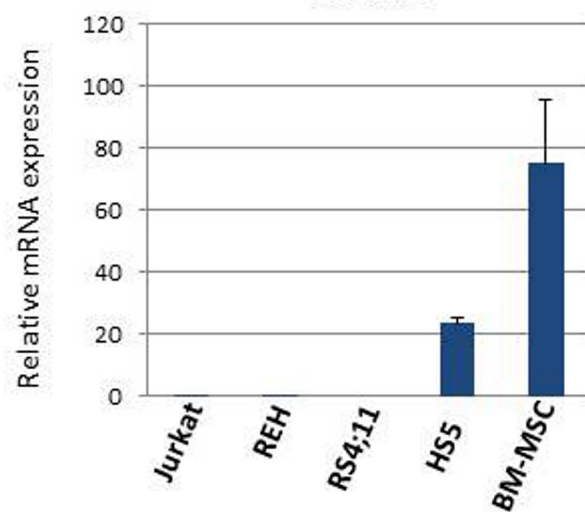
## CTGF



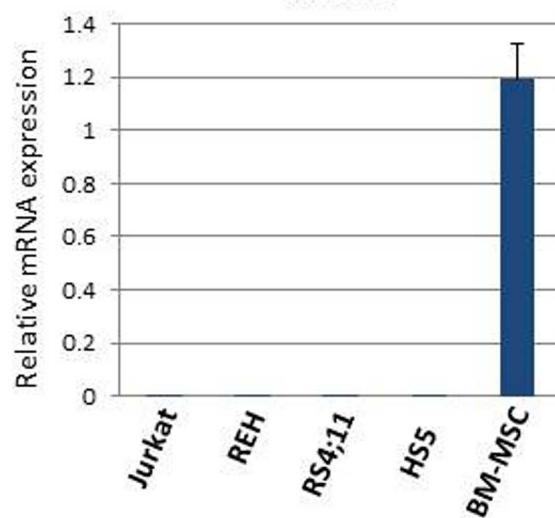
## WISP1



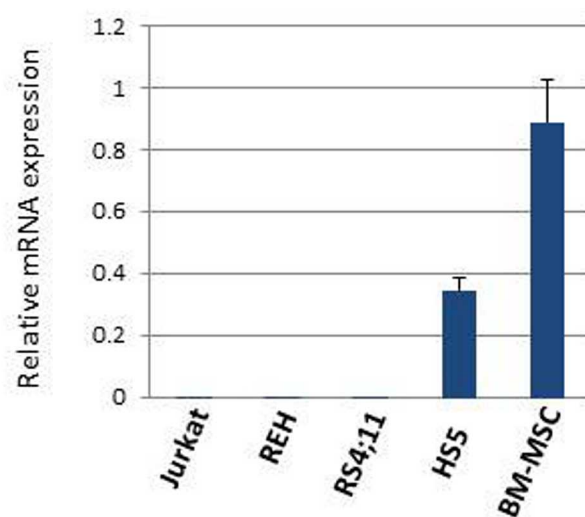
## CYR61



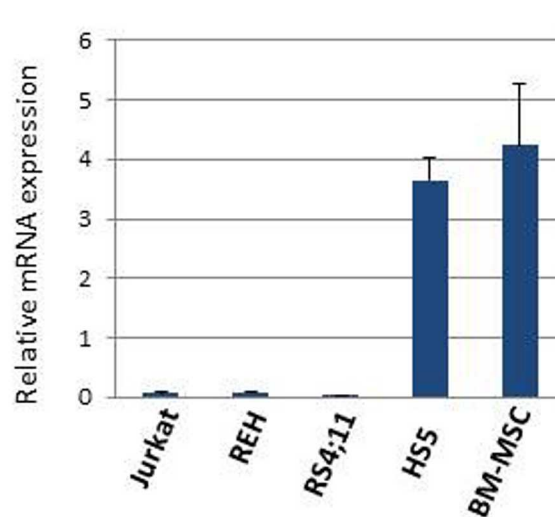
## WISP2



## NOV



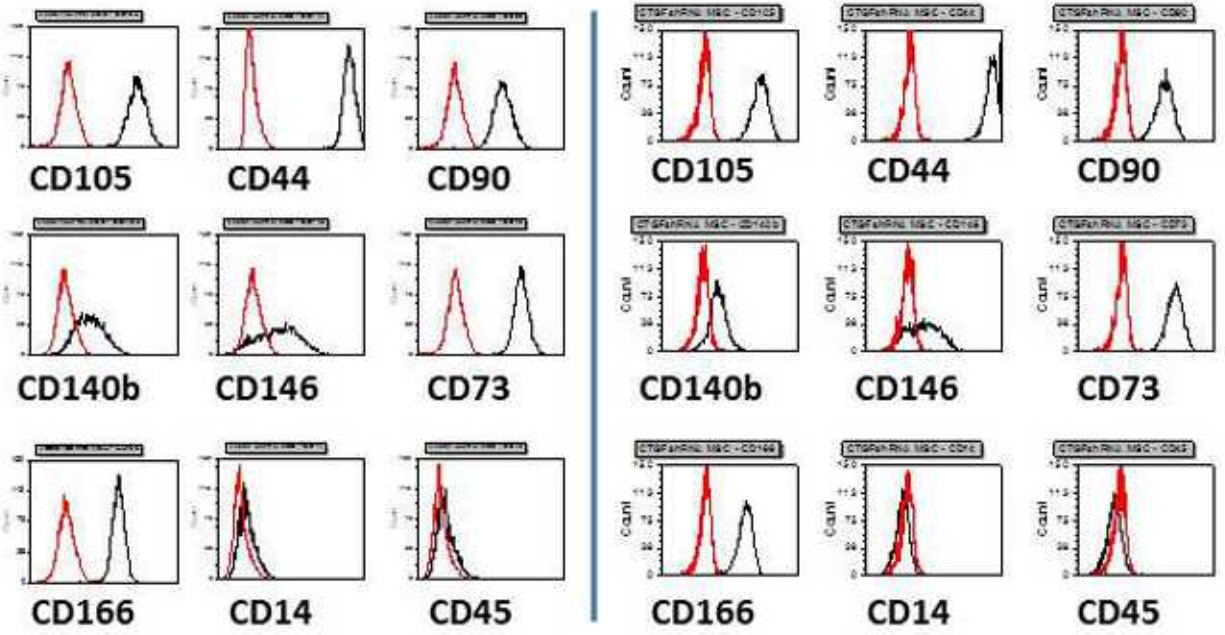
## LRP1



Cell surface phenotype

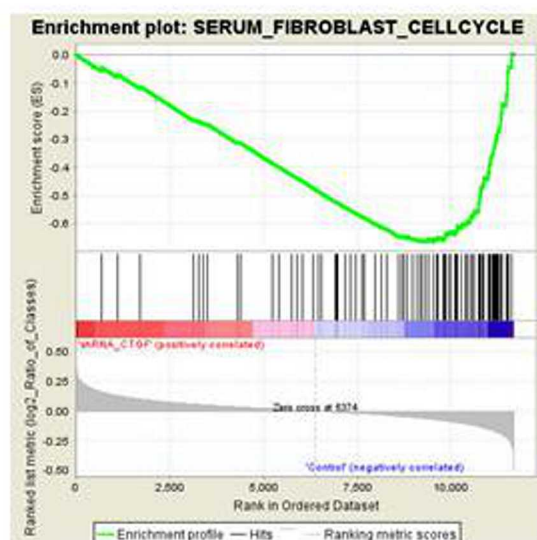
Control MSCs

CTGF-KD-MSCs



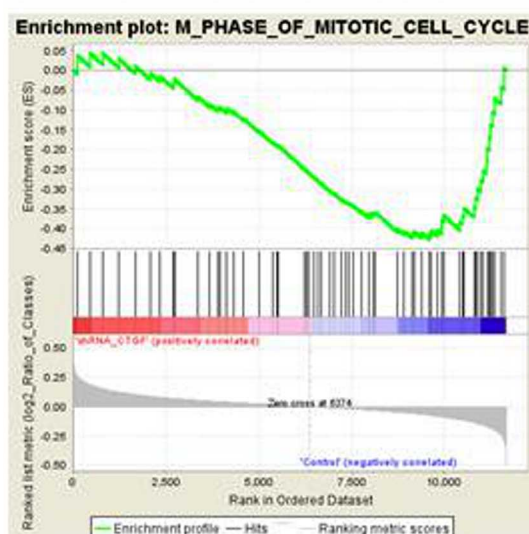
A)

Cell proliferation

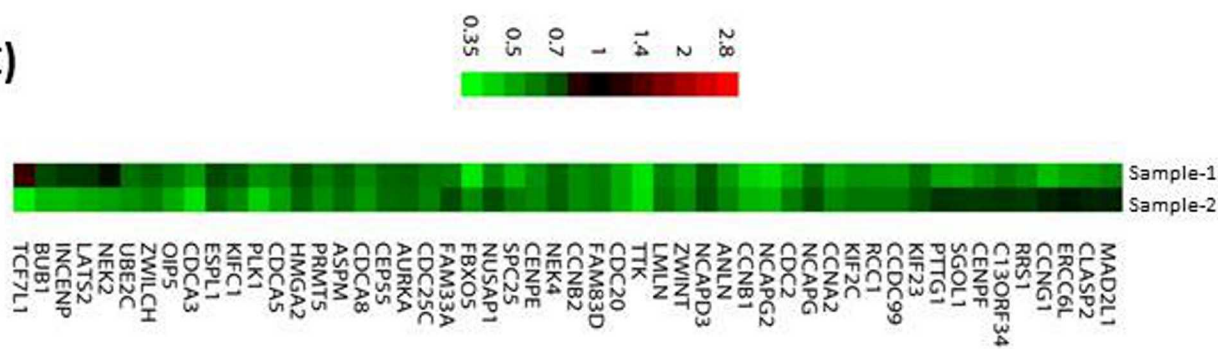


B)

M phase of mitotic cell cycle

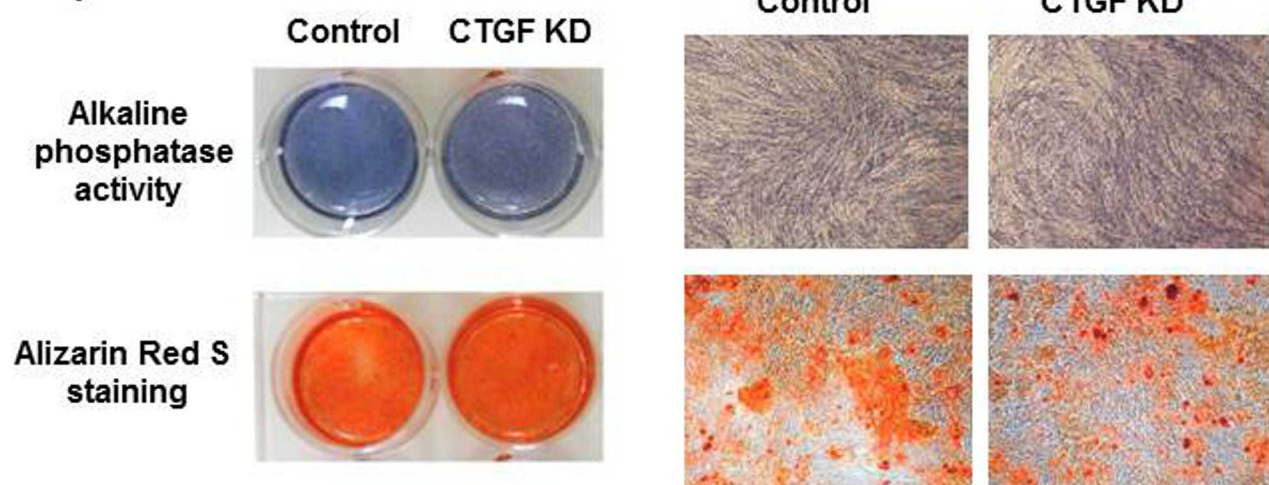


C)

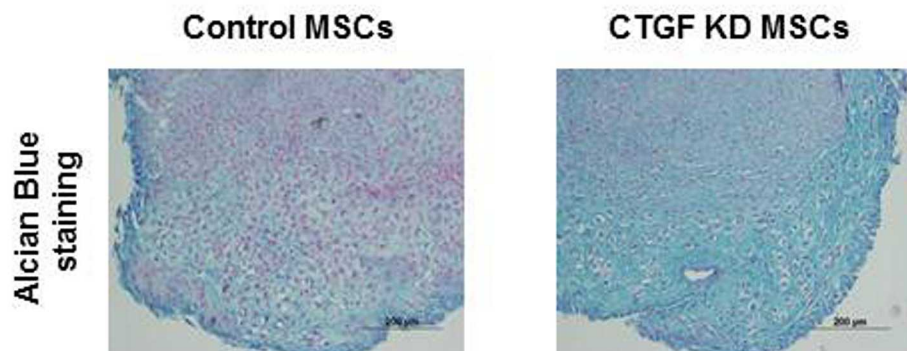


# Supplementary figure -4

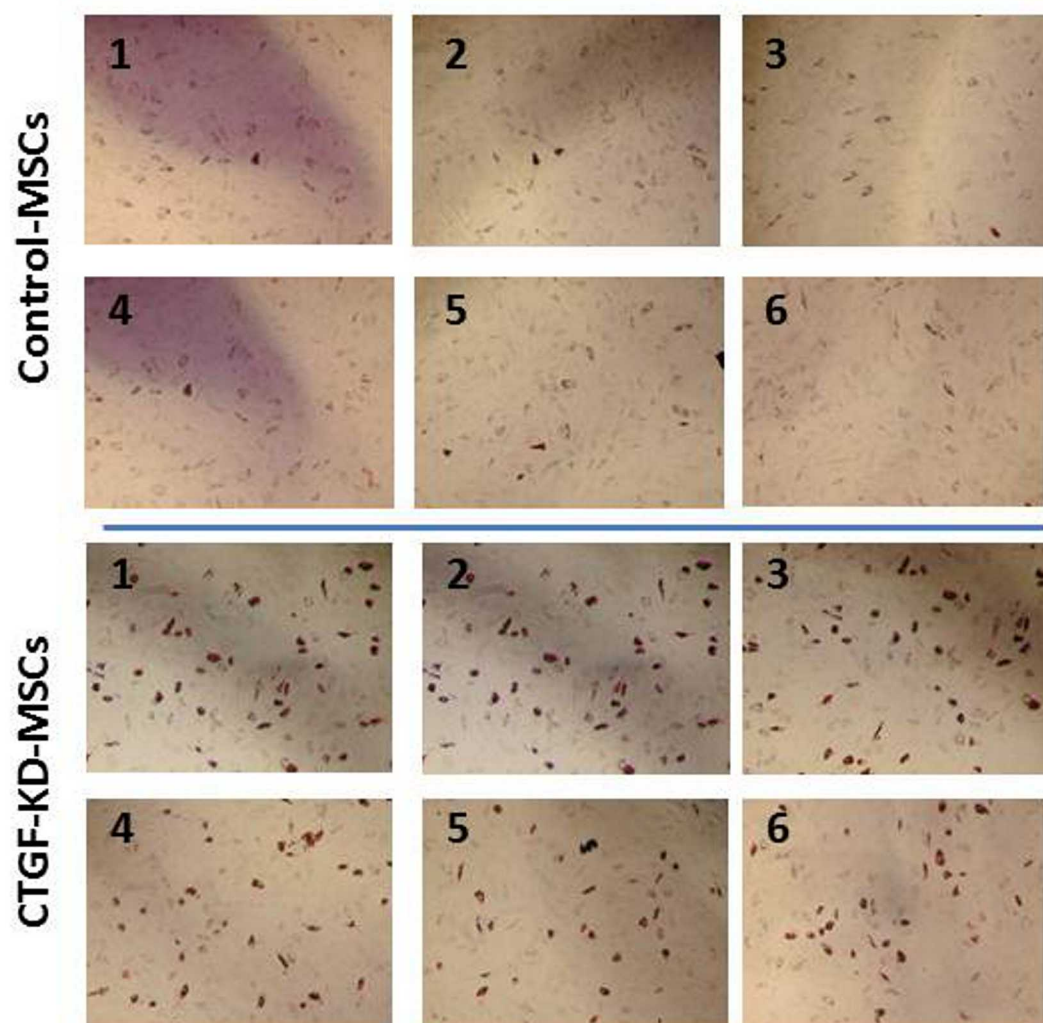
**A)**



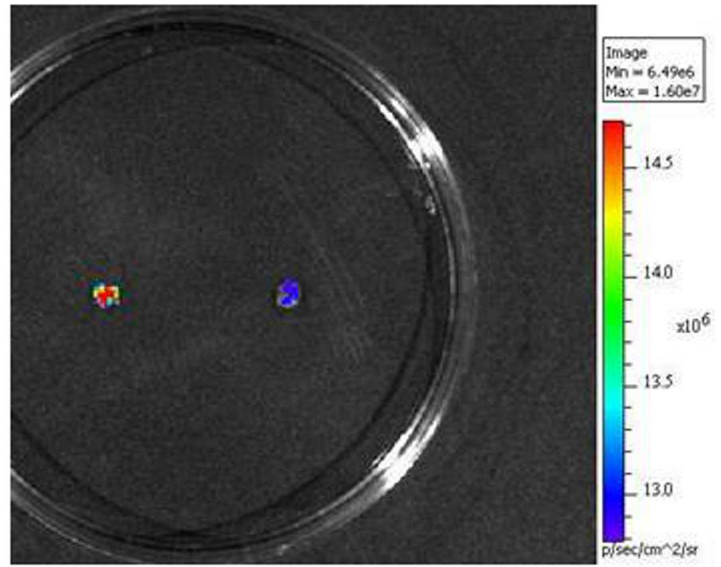
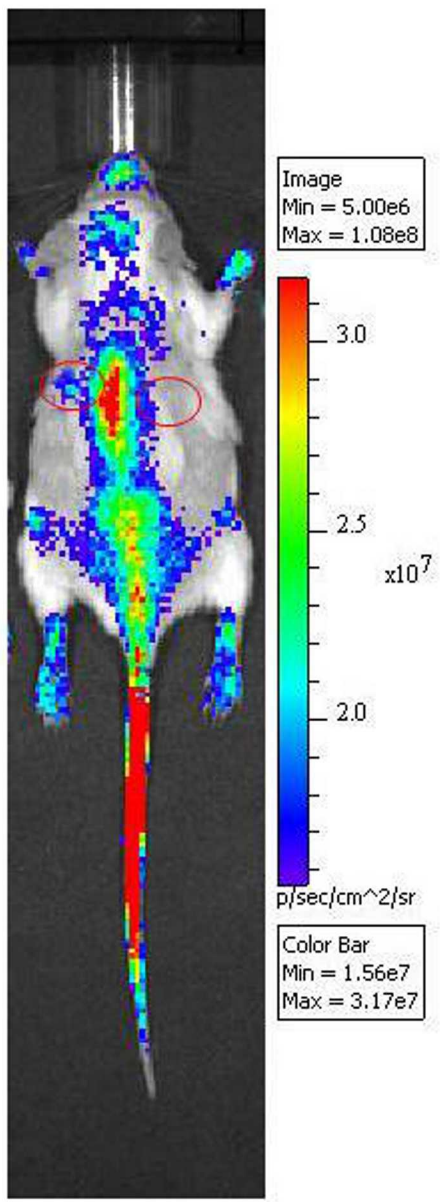
**B)**



### Adipocyte differentiation

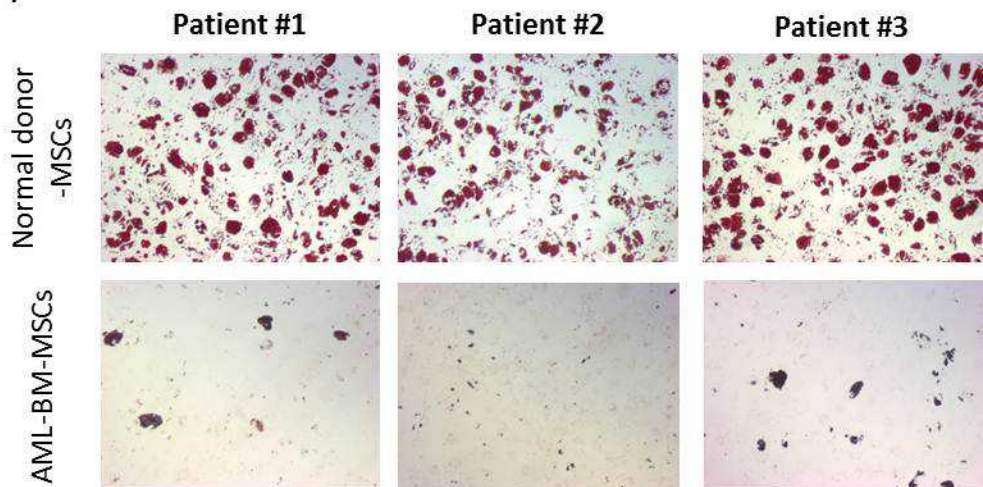


# Supplementary figure -6



# Supplementary figure 7

A)



B)

